A Meteorological Indicator for Particulate Matter Emissions: Adapting the Hot-Dry-Windy Index to Predict Feedlot Evening Dust Peaks

Sirapoom Peanusaha[a*], Guillermo Marcillo[b], Brent W. Auvermann[a]

[a] Texas A&M AgriLife High Plains Research and Extension Center, 3211 Russell Long Blvd., Canyon, TX, 79015 United States of America

[b] West Texas A&M University, 335 HSB Academic & Research Bld., Canyon, TX 79016 United States of America

[*] Corresponding author for preprint version

Abstract

Particulate matter emissions from cattle feedlot operations pose significant challenges to both livestock productivity and air quality in surrounding communities. The evening dust peak (EDP) has been documented for decades, but comprehensive long-term studies examining its meteorological drivers are very limited. While laboratory and field-scale investigations have demonstrated that feedlot surface moisture strongly influences dust emissions, direct moisture measurements are labor-intensive, limiting their operational utility. This study presents a novel framework for estimating feedlot surface moisture conditions using readily available meteorological data by adapting the Hot-Dry-Windy Index (HDW). An empirical water balance model integrating HDW with precipitation inputs was developed to characterize the dynamic interplay between atmospheric drying demand and moisture availability. Under the driest surface conditions, HDW explained 43% of the variability in evening PM_{10} concentrations ($R^2 = 0.433$, $r = 0.658$, $p < 0.001$),

demonstrating substantial predictive capability when atmospheric drying demand is the primary driver of emission potential. Using a comprehensive 10-year dataset, we quantified EDP characteristics and their relationship with meteorological conditions. Results confirm that the dust concentration in the evening hours consistently contributes 40-60% of 24-hour cumulative emitted mass of PM_{10} concentration. Analysis of atmospheric stability effects, characterized by vertical temperature gradients, revealed that temperature inversion alone cannot cause elevated dust concentrations but rather modulate the dispersion of emissions driven primarily by animal activity. These findings indicate that robust operational dust prediction models require animal activity parameters to describe emission mechanisms comprehensively.

Keywords: Cattle, feedlot dust, particulate matter, hot-dry-windy index, evening dust peak, atmospheric stability

1. Introduction

The cattle feedlot industry represents a critical economic driver in the Texas Panhandle economy, generating up to $3.1 billion annually and employing approximately 54,000 workers (Jones et al., 2024). Particulate matter (PM) emissions from feedlot operations pose significant challenges to both animal health and human welfare. Within feedlots, elevated PM_{10} (PM with aerodynamic equivalent diameter < 10 μm) concentrations adversely affect cattle health, causing respiratory diseases such as pneumonia (MacVean et al., 1986; Razote et al., 2008), which costs beef producers up to $900 million annually (Urso et al., 2021). Respiratory diseases attributable to excessive dust exposure account for approximately three-quarters of feedlot morbidity (Loneragan et al., 2001), representing substantial economic losses beyond production costs. For communities

located in proximity to feedlot operations, PM_{10} poses public health concerns due to its ability to penetrate and deposit within the human respiratory system (Arias-Pérez et al., 2020; Emert et al., 2023).

Chronic exposure to elevated PM_{10} concentrations has been linked to a range of adverse health outcomes, including respiratory and cardiovascular diseases, cancer, systemic inflammation, and reduced life expectancy (Mukherjee and Agrawal, 2017). The National Ambient Air Quality Standards (NAAQS) established a regulatory limit for PM_{10} of 150 $\mu g/m^3$ as a 24-hour average (USEPA, 2024) , applicable to all emission sources. In this context, effective dust management strategies for feedlot operations are of shared interest among multiple stakeholders. Economically, improved dust control may reduce animal health costs associated with respiratory diseases while demonstrating environmental stewardship by reducing nuisance conditions. For surrounding communities, effective dust management enhances air quality and quality of life. Regulatory compliance with government air quality standards protects both public health and the industry's public image.

Effective dust management in feedlot operations requires a comprehensive understanding of the trends of particulate matter emissions, particularly given that the magnitude of fugitive dust from feedlots has been disputed for more than three decades (Auvermann et al., 2010). Despite variability in reported emission magnitudes across studies, one phenomenon has been consistently documented in feedlot PM research: the evening dust peak (EDP). The EDP is characterized by a sharp spike in PM_{10} concentrations during evening hours (Auvermann et al., 2010; Bonifacio et al., 2013a, 2012, 2011; Emert et al., 2024; Hiranuma et al., 2011; McGinn et al., 2010; Razote et al.,

2008; Sweeten et al., 1998). This phenomenon is commonly attributed to the convergence of three meteorological and behavioral factors: increased animal activity during evening feeding times, peak manure surface dryness following afternoon drying, and the development of temperature inversions that suppress vertical mixing and trap dust emissions in the lower atmospheric boundary layer (Auvermann et al., 2010; Bush et al., 2014; Emert et al., 2024). The magnitude of the EDP can be substantial, with Auvermann et al. (2010) noting that evening PM_{10} concentrations can reach 10 to 15 times the 24-hour daily average value. Multiple studies have consistently reported EDP concentrations in the range of 400 to 2,000 $\mu g/m^3$ based on an hourly average (Bonifacio et al., 2011; Emert et al., 2024; Hiranuma et al., 2011).

Substantial research has been conducted to identify factors governing feedlot dust concentrations and develop mitigation strategies. Laboratory-scale investigations have established fundamental relationships between surface conditions and dust emission potential. Razote et al. (2006) demonstrated that feedlot surface moisture content is inversely related to dust emission potential, while animal trampling force shows a positive correlation with dust generation. Building on this understanding, Guo et al. (2011a) tested surface modification strategies at the laboratory scale, finding that adding hay to feedlot surfaces could reduce dust emission potential by approximately 77%.

Field-scale mitigation studies have evaluated the effectiveness of various dust control measures under operational conditions. Bonifacio et al. (2011) quantified the impact of sprinkler irrigation on PM_{10} emissions, demonstrating reduction efficiencies of 32% to 80%, though the suppression effect lasted only one day or less. Notably, this study also revealed that natural precipitation events produced superior dust control (60% to nearly

100% reduction) with suppression effects persisting for 3 to 7 days depending on rainfall amount and intensity. From a management perspective, Bush et al. (2014) demonstrated that increasing stocking density, which reduces individual animal activity and increased moisture-deposition flux through space limitation, shows potential for decreasing dust emission flux from feedlot operations.

Guo et al. (2011b) conducted a comprehensive 3-year study at two large feedlots (25,000 to 30,000 head capacity) using intensive monthly sampling campaigns (3–5 days per month) with gravimetric samplers. This investigation identified a critical surface moisture threshold of approximately 20%, above which PM_{10} concentrations decrease significantly. This threshold value provides an important benchmark for operational dust management strategies.

While these previous studies have established foundational understanding of feedlot dust dynamics, several areas warrant further investigation to advance both scientific understanding and operational applications. The EDP phenomenon, though consistently observed across multiple studies, has primarily been characterized qualitatively rather than quantitatively in long-term datasets. Sampling methodologies employed in many studies, such as the gravimetric samplers used by (Guo et al., 2011b; Habib et al., 2024), produce 10- or 12-hour average concentrations that inherently smooth out short-duration peak events. Similarly, studies by (Bonifacio et al., 2013b, 2011; Hiranuma et al., 2011) describe EDP qualitatively to explain observed dust spikes, but the temporal resolution and duration of available datasets have limited comprehensive analysis of the meteorological drivers' consistency and the frequency with which EDP significantly contributes to daily dust loads. Understanding the temporal persistence and relative

contribution of EDP to total daily emissions would enhance predictive capabilities and inform targeted management strategies.

The critical moisture threshold of 20% identified by Guo et al. (2011b) and Bonifacio et al. (2013b) represents an important contribution to feedlot dust management. However, validation of this threshold across diverse feedlot settings would strengthen confidence in its universal applicability. Additionally, the direct feedlot surface sampling approach employed in these studies is labor-intensive and raises questions about spatial representativeness given the heterogeneity typical of feedlot surfaces (Diller et al., 2026). This limitation highlights the need for alternative approaches to characterize surface moisture conditions across operational timeframes.

An opportunity exists to develop methodologies that leverage readily available meteorological data from on-site weather stations to estimate feedlot surface moisture content continuously. While Marek (2006) pioneered efforts to use reference evapotranspiration (ET_0) for estimating feedlot moisture dynamics, their results revealed significant discrepancies between standard ET_0 calculations and actual feedlot evaporation rates because the ET_0 approach assumes energy limited dynamics rather than the water-limited condition typical of feedlot surface in the southern Great Plains.

The overarching goal of this study was to advance the understanding of the EDP phenomenon, its contribution to total feedlot dust emissions, and its interaction with meteorological conditions using a long-term dataset. To achieve that goal, three specific objectives were established. First, we characterized the consistency and magnitude of EDP across a 10-year continuous monitoring dataset (2011–2019) to quantify its temporal persistence and relative contribution to daily dust loads. Second, we developed an

empirical model to estimate feedlot surface moisture content using readily available meteorological variables establishing a foundation for future development of robust EDP magnitude prediction tools. Third, we analyzed seasonal patterns of EDP occurrence and magnitude in relation to their meteorological drivers.

2. Materials and Methods

2.1 Study Location

The study was conducted at a commercial cattle feedlot, designated as Feedyard-C (FYC) to maintain operational anonymity. This facility, with a capacity of approximately 50,000 heads of cattle, operates year-round and is representative of large-scale feeding operations in the region. Data collection at this site spanned from 2011 to 2019, providing an extended monitoring period that captured seasonal variations, inter-annual climate variability, and diverse operational conditions (Marcillo and Auvermann, 2025).

2.2 Instrumentation

Particulate matter measurements (PM_{10}) were obtained using tapered element oscillating microbalance instruments (TEOM Series 1400a; Thermo Fisher Scientific, East Greenbush, NY) deployed at multiple points upwind and downwind of the study feedlot. These instruments captured mass concentration readings every 5 minutes, with size-selective inlets mounted at 2.0 m height. Regular maintenance protocols included filter temperature management, leak testing, inlet sanitation, pump verification, flow rate validation, software calibration procedures, and filter cartridge replacement based on loading criteria, all conducted according to manufacturer specifications and established practices from comparable particulate matter investigations conducted by partner institutions (Auvermann et al., 2010; Bonifacio et al., 2012; Razote et al., 2008).

The monitoring configuration consisted of an upwind station positioned south of FYC to capture background concentration, situated away from unpaved roadways to minimize traffic-related interference. Six additional monitoring stations were distributed at 140 meter intervals along an east-west transect in a 9-acre grassland buffer zone adjacent to the facility's northern boundary. This spatial arrangement was designed to capture emissions transported by the region's characteristic summer wind patterns, which predominantly blow from the south-southwest to south-southeast quadrants, with occasional northerly flows during winter months.

Meteorological parameters were captured through multiple sensor systems. A Vaisala HMP-45 combination sensor (Vaisala, Vantaa, Finland), protected by a passively ventilated shield and positioned 1.5 m above grade, recorded temperature in degrees Celsius and relative humidity as a percentage. Temperature values represented instantaneous minute-averaged readings, while humidity calculations integrated vapor pressure measurements over each minute. An RM Young 3D Ultrasonic Anemometer Model 81000 V (R. M. Young Company, Traverse City, MI, USA) mounted at 10 m elevation captured wind velocity and direction at 10 Hz sampling frequency. One-minute wind speed averages (m/s) and vector-averaged wind directions (degrees from north) were computed from these high-frequency measurements. A Gill WindSonic 2D Sonic Anemometer (Gill Instruments, Hampshire, UK) at 2 m height provided supplementary wind speed (m/s) at 1 Hz, also averaged over one-minute intervals. Rainfall accumulation was quantified using a Hydrological Services TB3 Tipping Bucket rain gauge mounted at 1.8 m, with 1 mm resolution.

2.3 Data Preprocessing

PM_{10} and meteorological data used in this study were preprocessed following the comprehensive methodology described by Marcillo and Auvermann (2025) for the FYC dataset spanning 2011-2019. The preprocessing workflow included temporal alignment and verification of sampling intervals, quality control through rolling window standardization (7-day window, 3 standard deviation threshold) to address anomalies while preserving valid extreme events, gap-filling using polynomial interpolation for short discontinuities (Lepot et al., 2017), and temporal aggregation to hourly and daily resolutions using a median point-estimate to remove outliers. These quality-controlled, aggregated datasets constitute the foundation for subsequent analysis in this study.

2.3.1 Upwind-Downwind Station Configuration and Net Concentration Calculation

Due to the predominant southerly wind direction (Figure 1), the upwind TEOM station was positioned at the southern end of the feedlot, with six downwind TEOM stations arranged in a linear array at the northern end. Summer and fall exhibit predominant southerly winds (>40% frequency), creating favorable conditions for measuring net feedlot emissions with the upwind-downwind station configuration. In contrast, spring shows more variable wind patterns with reduced southerly wind dominance, while winter displays the most dispersed wind distribution across all cardinal directions. These seasonal wind patterns directly influenced data availability, with summer and fall providing substantially more usable measurement periods compared to winter and spring. These downwind stations were placed perpendicular to the expected plume trajectory. Net concentrations attributable to feedlot emissions were calculated by subtracting

upwind concentrations from downwind measurements. Since six downwind stations were deployed, six net concentration values were available at each 1-hour interval.

To ensure statistical reliability and data visualization clarity, concentration values were capped at 3,000 μg/m³, preventing anomalously high readings (>10,000 μg/m³) from skewing the results (Emert et al., 2024). Each hourly measurement was flagged as usable or unusable based on wind direction criteria. Data was considered usable when wind direction remained within +/- 45° of due south; otherwise, net concentration values were marked unusable, as the downwind TEOM stations would not capture the main body of the dust plume under those conditions.

The dataset comprised 3,282 days with concurrent meteorological and PM_{10} concentration measurements. Of these, 569 days had ≥18 hours of valid data (≥75% daily PM_{10} concentration data availability), meeting the threshold for complete daily data ("WMO Guidelines on the Calculation of Climate Normals_en," 2017), while 1,026 days had ≥6 hours of valid evening data between 16:00 and 24:00 (≥75% evening data availability). Days with complete data availability occurred predominantly during summer and fall, whereas spring and winter exhibited substantially fewer usable measurements due to a higher frequency of westerly winds (see Figure 2). In Figure 2, the heatmap (top) displays the number of days per month with ≥18 hours of valid net concentration data, with darker shading indicating higher data availability. The bar chart (bottom) shows seasonal data availability, with summer exhibiting the highest proportion of usable data (31.1%), followed by fall (19.2%), spring (14.9%), and winter (6.0%). Usable data were distributed uniformly across years, except for 2016, which shows notably

reduced data availability due to sensor malfunction. White cells indicate months with no valid measurements meeting the threshold criteria.

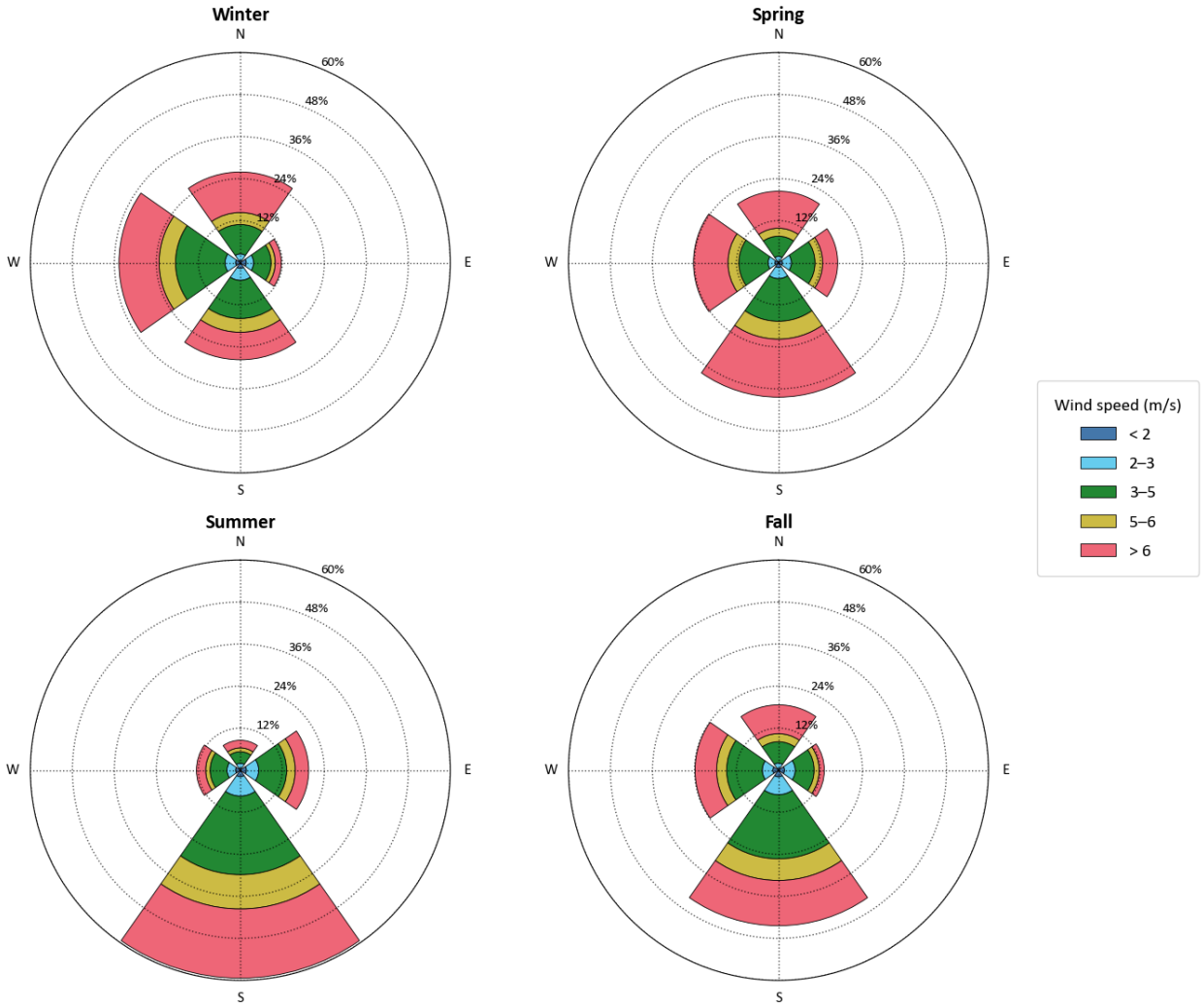

Figure 1. Seasonal wind rose diagrams showing wind speed and direction frequency at the feedlot study site (2011–2019).

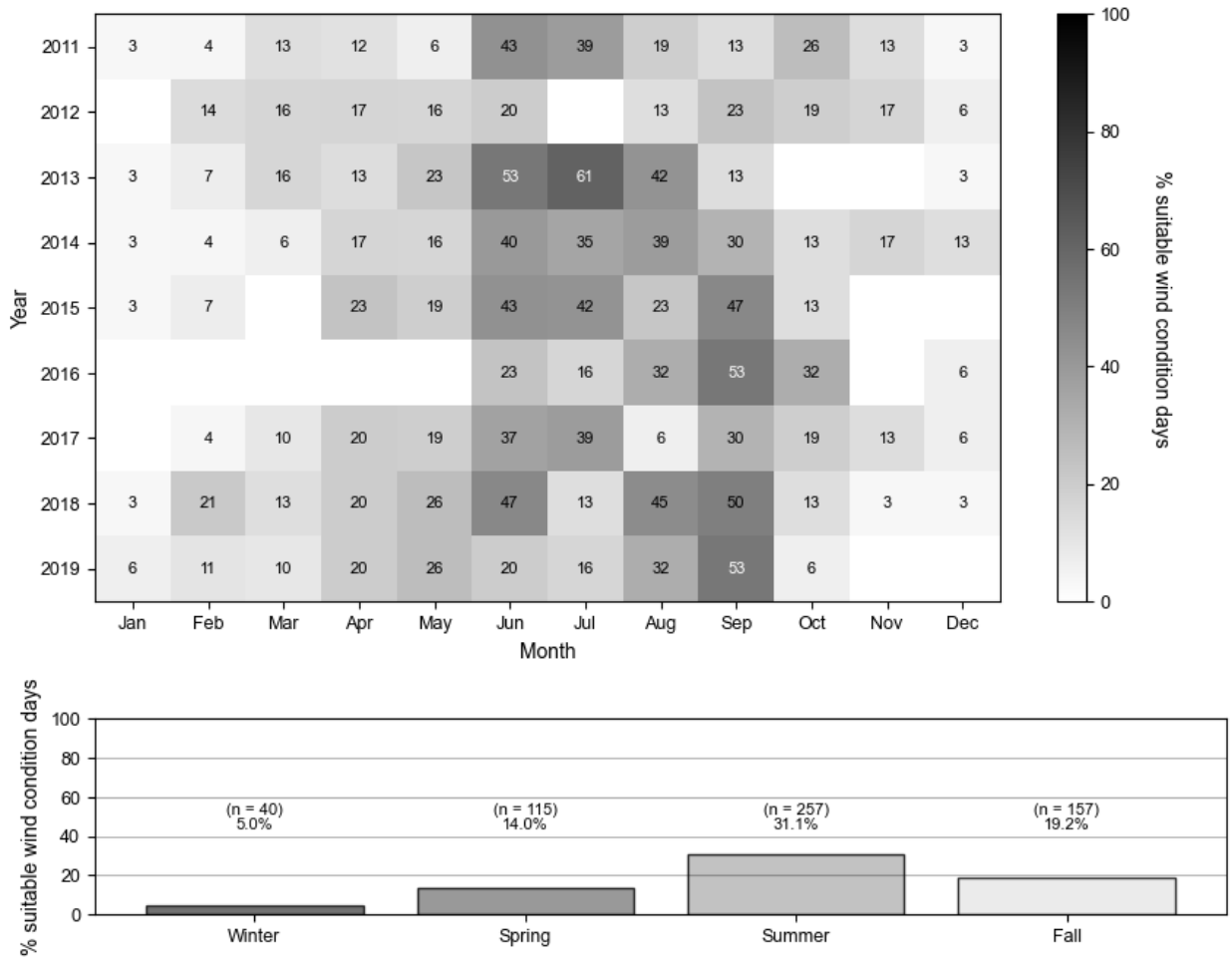

Figure 2. Temporal distribution of usable PM_{10} concentration data based on southerly wind conditions (2011–2019).

2.4 Meteorological Factor Derivation

2.4.1 Hot-Dry-Windy Index (HDW)

The Hot-Dry-Windy Index (HDW) is a meteorological index that combines vapor pressure deficit (VPD) and wind speed to assess atmospheric conditions that contribute to hazardous wildfire behavior (McDonald et al., 2018; Srock et al., 2018). HDW was specifically designed as a fire weather index that synthesizes basic meteorological variables (temperature, humidity, and wind speed) to identify days when specific weather

processes create conditions that make fires difficult to manage. The index has demonstrated utility in identifying anomalous atmospheric conditions, which provides locally and seasonally relevant context for determining high risk days. HDW has been used beyond wildfire applications to evaluate hot weather trends and their impacts on soil moisture availability in agricultural systems (Feng et al., 2026; Zhang et al., 2025). In the context of our feedlot dust emissions study, HDW is particularly applicable. This index captures the same atmospheric drivers that govern dust emission potential. VPD, which accounts for the evaporative demand of the atmosphere, directly relates to surface drying conditions that enhance dust generation from feedlot surfaces. Similarly, wind speed is critical for both initiating dust particle agitation and facilitating vertical dispersion of emitted particulates. Additionally, high wind speed also replace the dry air mass over an evaporating surface more frequently enhancing the effect of high VPD.

HDW in our dataset was calculated using hourly measurements of wind speed, relative humidity, and air temperature, providing a continuous metric to characterize the drying power exerted by atmospheric conditions on the feedlot surface. By adapting this proven methodology, we can objectively identify days when meteorological conditions favor elevated dust emission potential, independent of specific feedlot management practices or surface characteristics. HDW was calculated following:

$$\boldsymbol{HDW = VPD \times U} \quad \textbf{(1)}$$

where VPD is the vapor pressure deficit (kPa), representing the difference between saturation vapor pressure and actual vapor pressure, and U is wind speed (m s^{-1}) at 2-meter height. Saturation vapor pressure was calculated based on air temperature

measurements and relative humidity (Monteith and Unsworth, 2013), while actual vapor pressure was derived from relative humidity and barometric pressure observations.

2.4.2 Empirical Water Balance Model Development

HDW exhibited moderate correlation with daily and evening average PM_{10} concentrations, demonstrating its potential as a proxy for estimating the magnitude of EDP. However, certain days consistently deviated from this trend, particularly on days following recent rainfall events. This inconsistency highlighted the need to account for the competing effects of precipitation (moisture input) and atmospheric drying demand (moisture output) on feedlot surface conditions. Therefore, an empirical model was developed to integrate atmospheric drying power and precipitation inputs to monitor estimated surface moisture levels at the feedlot.

The model was developed based on a leaky bucket concept, where precipitation acts as moisture input, HDW represents atmospheric moisture demand (outflow), and daily moisture loss occurs through drainage and seepage. This approach was necessary to address a specific limitation identified during initial exploratory analysis. Early attempts to predict evening dust concentration peaks using simple multi-day cumulative sums of precipitation and HDW (up to 14-day cumulative) failed to account for the chronological sequence of meteorological events. For instance, a simple cumulative approach incorrectly assumes that high evaporative demand (HDW) occurring early in a given week can remove moisture from precipitation that occurs later in that same week, which is physically inaccurate. To resolve this temporal mismatch and accurately represent the moisture memory of the feedlot surface, a recursive daily water balance equation was developed that processes meteorological inputs in chronological order, ensuring that each day's moisture state depends only on prior conditions and current inputs as follows:

$$M_t = \gamma M_{t-1} + P_t - \beta E_{HDW,t} \quad (2)$$

where M_t is the surface moisture state on day t (dimensionless), M_{t-1} is the antecedent moisture condition from the previous day, P_t is daily total precipitation (mm), and $E_{HDW,t}$ is the daily cumulative HDW representing atmospheric drying potential. The persistence coefficient a ($0 < \gamma < 1$) governs the hydraulic memory of the feedlot surface, with higher values indicating greater moisture retention capacity. The drying coefficient β scales the HDW atmospheric demand to the equivalent rate of surface moisture depletion, enabling direct comparison between moisture inputs from precipitation and losses from evaporative demand. The persistence coefficient γ and drying coefficient β were derived through iterative optimization to maximize the correlation between modeled surface moisture and observed maximum evening PM_{10} concentrations. Parameter ranges were constrained based on physical considerations and the magnitude of daily cumulative HDW values. The optimization yielded γ = 0.9 and β = 0.0008, with an initial surface moisture condition of $M_0 = 0$ on January 1, 2011.

2.4.3 Vertical Temperature Gradient and Evening Boundary Layer Stability

Previous studies (Bonifacio et al., 2012; Muñoz and Corral, 2017) have mentioned that atmospheric stability during evening hours plays an important role in trapping fugitive dust within the boundary layer, contributing to EDP. Muñoz and Corral (2017) specifically reported a direct correlation between average PM_{10} concentration and the temperature gradient between 2- and 10-meter heights in an urban setting, which closely parallels the measurement configuration employed in this study. To characterize atmospheric stability conditions, we incorporated temperature gradient as a key parameter. Positive temperature gradients (temperature inversions) during evening hours suppress vertical

mixing and trap polluted air near the surface, enhancing dust accumulation at ground level. Conversely, negative temperature gradients indicate unstable conditions during which warmer surface air rises and mixes with cooler upper air, facilitating vertical dispersion of emitted dust. Following the methodology of Muñoz and Corral (2017), the temperature gradient was calculated as the difference between ambient air temperature at 10 meters and air temperature at 2 meters, divided by the vertical separation distance (8 meters), yielding a gradient in units of $°C\ m^{-1}$.

2.5 Statistical Analysis

A two-way analysis of variance (ANOVA) was performed to assess the effects of modeled surface moisture content and temperature gradient on evening dust concentrations. Both meteorological variables were categorized into quartiles to examine differences across moisture and stability regimes. The modeled surface moisture quartiles represented dry to wet conditions, while temperature gradient quartiles captured the range from strong inversions (stable conditions) to negative gradients (unstable conditions). Evening dust concentrations were log-transformed prior to analysis to meet ANOVA assumptions of normality and homogeneity of variance.

The two-way ANOVA tested for main effects of each factor as well as their interaction effect on log-transformed PM_{10} concentrations. Following significant ANOVA results, Tukey's Honestly Significant Difference (HSD) post-hoc test was conducted to identify which specific quartile groups differed significantly from one another. Statistical significance for all tests was declared at $\alpha = 0.05$ ($p < 0.05$).

3. Result and Discussion

3.1 Decadal Trends in EDP Magnitude and Contribution to Daily Dust Loads

Figure 3 displays the diurnal pattern of EDP aggregated from all data collected between 2011 and 2019.

The top panel displays monthly average PM_{10} concentrations. Monthly average PM_{10} concentrations are highest during spring and summer months, coinciding with elevated temperatures during this period. Paradoxically, these same months (May through August) also experience the highest rainfall, creating conditions characterized by high atmospheric heating potential, more frequent precipitation events, and elevated dust concentrations. The diurnal trends reveal that EDP timing closely follows seasonal sunset patterns, occurring when ambient air temperature stabilizes after declining from its midday maximum, relative humidity reaches its daily minimum, and wind speed tends to decrease. The timing of maximum EDP varies seasonally, typically occurring at 18:00 during winter and fall, shifting later to 19:00–20:00 during spring and summer as daylight hours extend and sunset occurs progressively later in the evening.

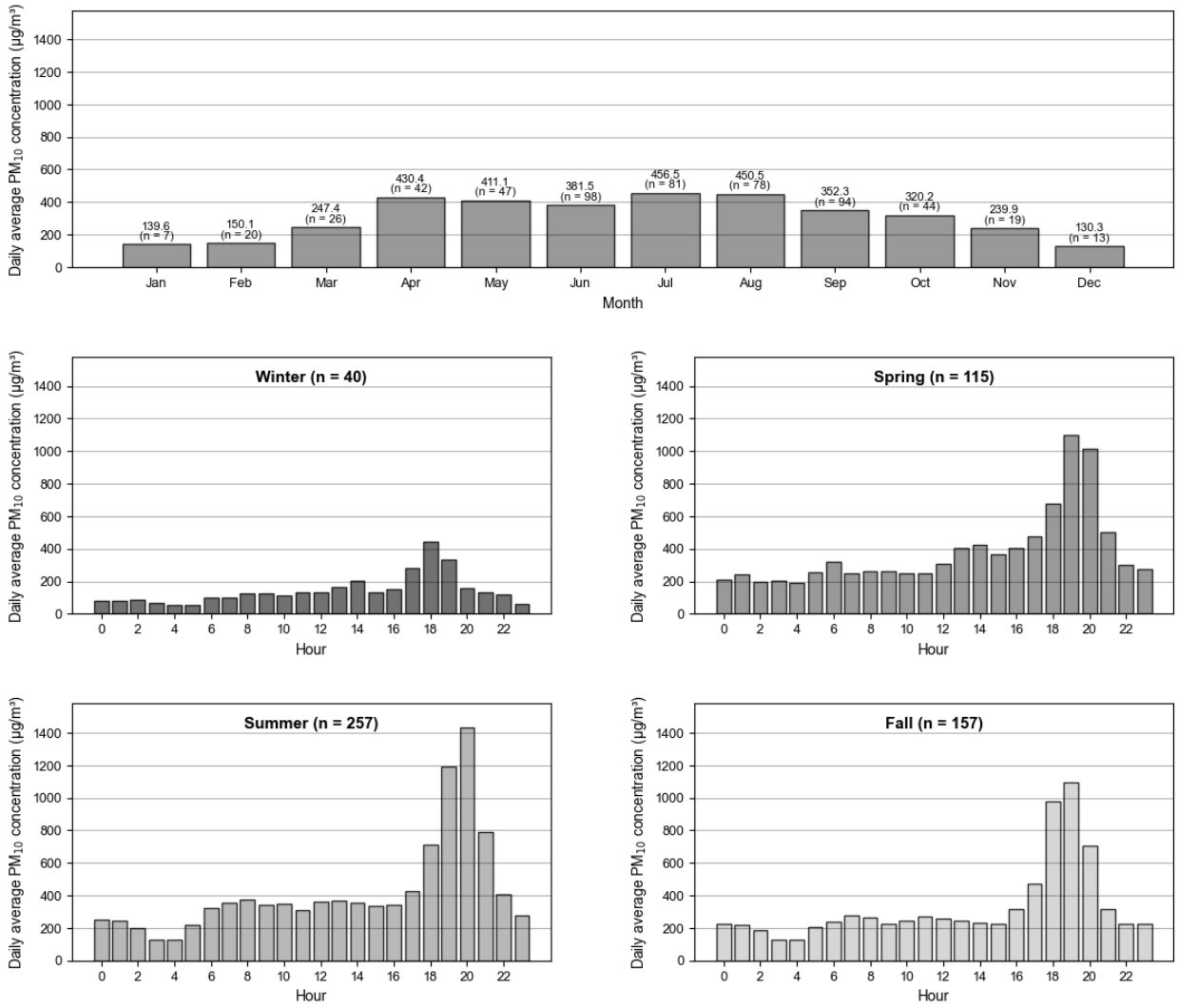

Figure 3. Seasonal diurnal patterns of net PM10 concentrations (2011–2019) showing consistent EDP across all seasons with timing correlated to sunset.

The temporal analysis reveals distinct seasonal patterns in the contribution of EDP to total daily PM10 emissions over the 10-year study period. Summer months consistently demonstrated that EDP contributed more than 50% to the magnitude of the 24-hour average PM10 dust load. Spring and fall exhibited more variable patterns, with EDP contributions fluctuating across years, though these seasons still registered substantially

higher EDP contributions to daily dust loads compared to winter. Winter showed the most pronounced departure from other seasons, with both EDP magnitude and daily average PM_{10} concentrations consistently lower than during other times of year (Figures 3 and 4). The average evening peak concentration during winter reached only approximately 500 $\mu g/m^3$, representing less than half the magnitude observed during spring, summer, and fall (1,200–1,400 $\mu g/m^3$). Across all seasons and years, EDP contributed an average of 40–50% of the total 24-hour PM_{10} dust load, underscoring the disproportionate importance of evening emissions in characterizing daily feedlot dust dynamics.

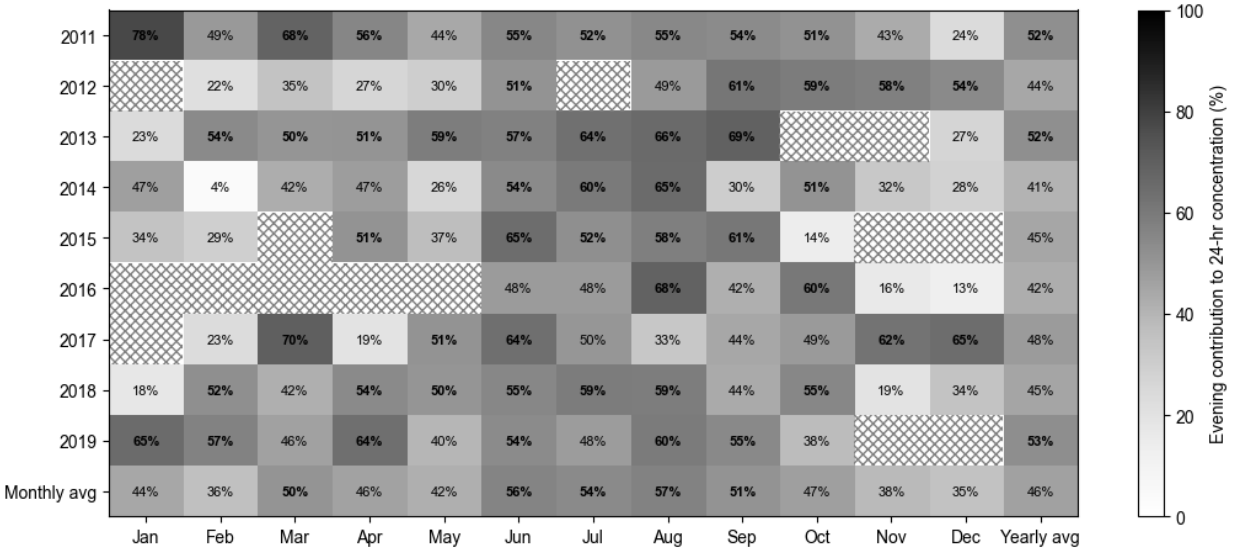

Figure 4. Annual and monthly contribution of evening PM_{10} concentrations (16:00–24:00) to 24-hour average PM_{10} magnitude showing EDP dominance during summer months. Percentages represent the proportion of daily dust load occurring during evening hours, with values >50% shown in bold. Hatched cells indicate insufficient data due to wind-direction constraints. Evening contributions

averaged 45–50% annually but increased substantially during June–September, consistently exceeding 50% and reaching 68% in August 2016.

3.2 Surface Moisture Modeling Using HDW and Precipitation Data

Figure 5 illustrates the complex interaction between precipitation timing (days since last rain) and atmospheric drying potential (daily accumulated HDW) on evening PM_{10} concentrations. The heatmap reveals that this relationship varies substantially depending on the magnitude of atmospheric drying demand. Under low HDW conditions (Q1), evening concentrations exhibit a highly variable pattern across different dry periods, with no clear monotonic trend as days since rainfall increase.

In contrast, under moderate to extreme HDW conditions (quartiles 2–4, HDW > 29), a more systematic pattern emerges. Evening PM_{10} concentrations increase progressively with both higher accumulated HDW values and longer periods since the last rainfall event, indicating that strong atmospheric drying potential consistently enhances dust emissions, particularly when combined with extended dry periods. The highest concentrations (>1,200 $\mu g/m^3$) occur under extreme HDW conditions (Q4) combined with extended dry periods (>20 days since rain), demonstrating the compounding effects of prolonged surface drying and high atmospheric demand.

However, the variability observed within each category, particularly in the lower HDW quartiles, highlights a fundamental limitation of this simple two-parameter approach. The "days since last rain" metric alone provides a limited representation of feedlot surface moisture availability because it ignores critical factors such as precipitation amount,

antecedent moisture conditions from earlier rainfall events, and the temporal dynamics of moisture depletion.

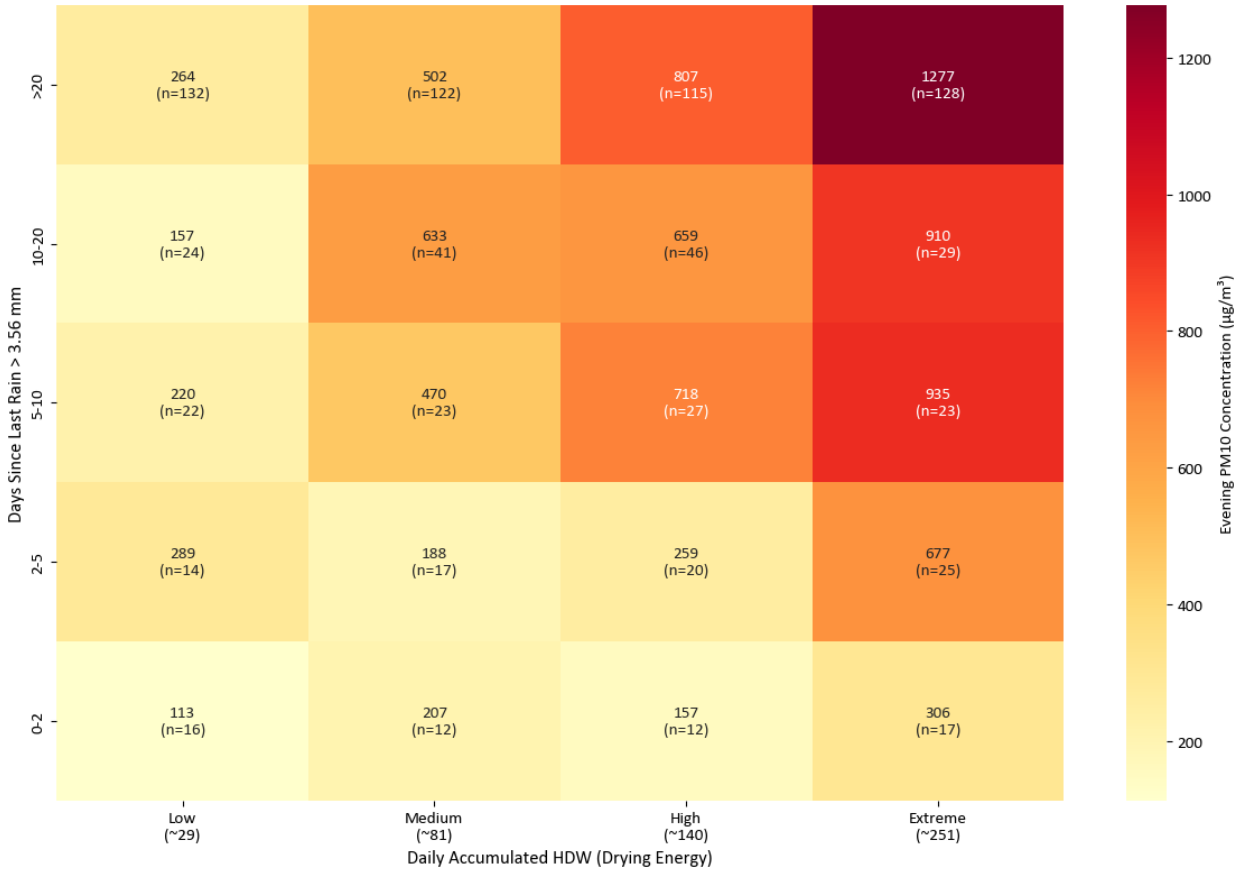

Figure 5. Interaction effects of precipitation timing and atmospheric drying potential (HDW) on evening PM_{10} concentrations. Heatmap cells show mean concentrations (µg/m³) grouped by days since last rainfall (>3.56 mm, representing the median precipitation amount across all rainfall events from 2011–2019) and daily accumulated HDW quartiles.

The empirical water balance model effectively captured the complex interaction between atmospheric drying potential and surface moisture (see Figure 6). The analysis reveals a systematic, moisture-dependent degradation in the relationship between daily

accumulated HDW and evening PM_{10} concentrations across the four surface moisture quartiles. Under the driest surface conditions (Q1), HDW exhibits strong explanatory capability for evening dust concentrations, with Pearson's r = 0.658 and R^2 = 0.433. However, as modeled surface moisture content increases from Q1 through Q4, both the correlation strength and explanatory power of HDW decline systematically (Q2: r = 0.506, R^2 = 0.256; Q3: r = 0.444, R^2 = 0.197; Q4: r = 0.327, R^2 = 0.107). This progressive weakening of the HDW-dust relationship with increasing surface moisture demonstrates the dominant role of surface wetness in suppressing dust emissions, even under meteorologically favorable conditions for dust generation. The reduction in explained variance from 43.3% to 10.7% between the driest and wettest quartiles quantifies the magnitude of this moisture suppression effect. These results validate the utility of the recursive water balance approach for integrating precipitation and atmospheric drying dynamics and demonstrate that readily available meteorological measurements from on-site weather stations (wind speed, relative humidity, air temperature, and precipitation) can be effectively synthesized to monitor and predict feedlot dust emission potential. The framework provides a practical tool for characterizing emission conditions using standard meteorological infrastructure without requiring direct soil moisture measurements.

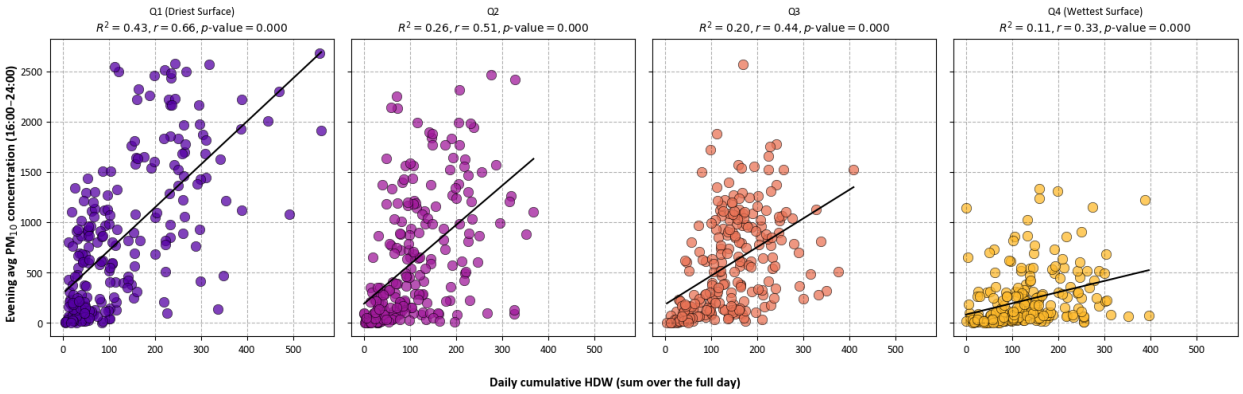

Figure 6. Effect of surface moisture on the HDW-PM_{10} relationship across moisture quartiles (Q1 = driest to Q4 = wettest). Linear regression analyses and Pearson's correlation show that the relationship between daily cumulative HDW and evening average PM_{10} concentrations systematically decreases with increasing surface moisture.

3.3 Influence of Vertical Temperature Structure on Evening Dust Peak Characteristics

Figure 7 reveals the atmospheric mechanism underlying the synchronization between EDP and temperature gradient development across all seasons. As sunset approaches, radiative cooling causes the feedlot surface to lose heat more rapidly than the overlying air mass, creating a thermal stratification where air temperature at 10 m exceeds temperature at 2 m. This temperature inversion structure suppresses vertical mixing and effectively traps dust particles emitted from animal activity within the lower atmospheric boundary layer, resulting in elevated PM_{10} concentrations measured at ground level (Olofson et al., 2009). The timing of both temperature gradient maxima and EDP exhibit strong correlation with seasonal sunset patterns: winter shows peaks occurring around 18:00, while spring and summer display progressively later peaks at 19:00 and 20:00 respectively, consistent with extended daylight hours during warmer months. The magnitude of temperature inversion remains relatively consistent across seasons (peak values ~0.2 to 0.3°C m^{-1}). Temperature gradient (blue line, °C m^{-1}) transitions from negative values during daytime (indicating unstable conditions with warmer air near the surface) to positive values during evening hours (indicating stable temperature inversion conditions). Net PM_{10} concentrations (red line, $\mu g/m^3$) remain relatively low and stable

during daytime hours across all seasons, then increase sharply during evening hours, peaking simultaneously with or within ±1 hour of the temperature gradient maximum.

Notably, the relationship between atmospheric stability and dust concentration exhibits asymmetric behavior during the diurnal transition periods. During morning hours, when the temperature gradient transitions from positive (stable inversion) to negative (unstable conditions with surface heating), PM_{10} concentrations do not immediately decrease to their daily minimum. Similarly, following the evening EDP maximum, concentrations decline gradually despite the persistence of positive temperature gradients that flatten around midnight. Across all seasons, minimum PM_{10} concentrations consistently occur between 02:00 and 04:00.

The temporal pattern shows that EDP consistently occurs shortly before the temperature gradient reaches its maximum. This temporal pattern suggests that dust emissions begin accumulating as atmospheric stability develops but before full inversion strength is achieved. Seasonal differences in distribution width are apparent, with fall and winter exhibiting significantly broader, more dispersed lag distributions compared to the concentrated patterns observed in Spring and Summer. This seasonal variation reflects data characteristics rather than underlying physical processes: during Fall and Winter, EDP magnitudes are substantially lower and less pronounced (as shown in Figures 3 and 7), making the identification of a distinct "peak" time more ambiguous. The absence of a single dominant evening concentration maximum during these seasons results in greater temporal variability in the recorded peak times, producing the wider lag distributions observed in Figure 7.

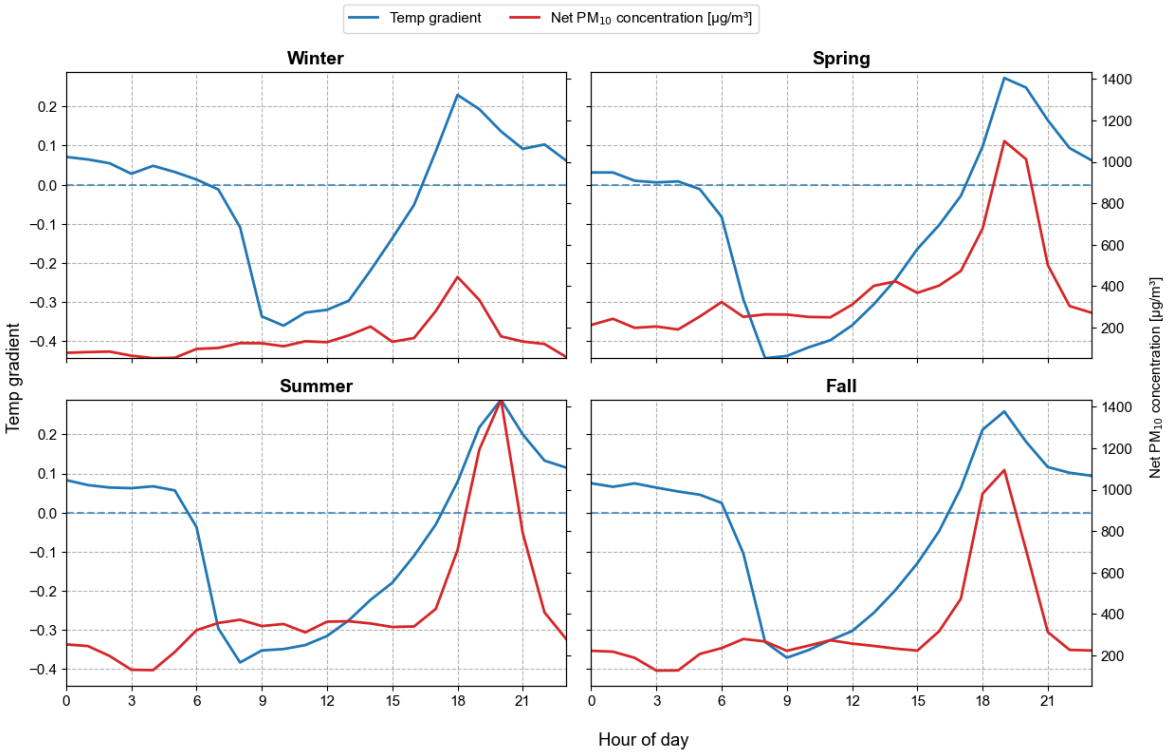

Figure 7. Seasonal diurnal patterns of temperature gradient (2 m to 10 m) and net PM10 concentrations showing synchronized evening peaks coinciding with sunset and temperature inversion development.

Figure 8 presents the seasonal diurnal patterns of evening PM10 concentrations stratified by atmospheric stability regime, where unstable conditions (Q1, red line) are characterized by negative or weakly positive temperature gradients that promote vertical mixing, and stable conditions (Q2–Q4 combined, blue line) represent moderate to strong temperature inversions that suppress dispersion. The 95% confidence intervals (shaded regions) show noticeable separation between EDP magnitudes under stable versus unstable conditions. Winter, spring, and fall exhibit pronounced separation between stable and unstable conditions, with non-overlapping confidence intervals indicating statistically significant differences in evening PM10 levels between the two stability

regimes. Under stable conditions during these seasons, evening concentrations reach substantially higher peaks (winter: ~650 μg/m³; spring: ~1,350 μg/m³; fall: ~1,100 μg/m³) compared to unstable conditions (winter: ~350 μg/m³; spring: ~800 μg/m³; fall: ~500 μg/m³). The more frequent occurrence of unstable temperature gradient conditions during winter and fall contributes to the robust contrast observed in these seasons. Winter displays the smallest sample size overall due to reduced frequency of southerly winds during this season, which limited the ability of the upwind-downwind TEOM station array to capture net feedlot emissions.

In contrast, summer shows substantially overlapping confidence intervals between stable and unstable conditions, indicating less distinct differences between the two atmospheric stability regimes during this season. The binary classification of stability (Q1 versus Q2–Q4) was adopted because PM_{10} concentrations did not increase proportionally with temperature gradient magnitude within the stable regime. Specifically, quartiles Q2, Q3, and Q4 did not exhibit a consistent progressive increase in average evening dust concentrations, suggesting that atmospheric stability operates as a threshold phenomenon rather than a continuously scaled effect: once inversion conditions establish (transition from Q1 to Q2), further increases in inversion strength produce diminishing effects on dust concentration near the ground surface.

Atmospheric stability regime and modeled surface moisture content exerted significant independent effects on evening PM_{10} concentrations (see Table 1). Atmospheric stability was classified into two groups based on temperature gradient quartiles: unstable conditions (Q1, representing negative or weakly positive temperature gradients with enhanced vertical mixing) and stable conditions (Q2–Q4). Evening net PM_{10}

concentrations were log-transformed prior to analysis to satisfy ANOVA assumptions of normality and homogeneity of variance. The stability group factor (Q1 versus Q2–Q4) showed a highly significant main effect ($F = 111.75$, $p < 0.001$), as did the surface moisture quartile factor ($F = 86.25$, $p < 0.001$). Our conceptual framework illustrates the fact that EDP results from the combined effects of atmospheric conditions that trap emitted particulates (stability) and surface conditions that govern emission availability (moisture content).

Table 2 demonstrates that within each atmospheric stability regime, the dust suppression effects of surface moisture exhibit a threshold behavior rather than a linear response. Pairwise comparisons between the driest conditions (Q1) and moderately dry conditions (Q2) show no statistically significant differences in evening PM_{10} concentrations ($p > 0.05$) under both unstable and stable atmospheric conditions. This finding suggests that modest increases in surface moisture from extremely dry to moderately dry states are insufficient to substantially alter EDP magnitude. However, when surface moisture reaches higher levels (Q3 and Q4), significant dust suppression becomes evident. Comparisons between Q1 and Q3, and particularly between Q1 and Q4, reveal highly significant reductions in evening concentrations ($p < 0.001$). Notably, the magnitude of moisture-induced concentration reduction is most pronounced under unstable atmospheric conditions. Under unstable conditions, the difference between the driest (Q1) and wettest (Q4) surface states produces a mean reduction of 2.53 log units (~300 times), compared to 1.69 log units (~40 times) under stable conditions.

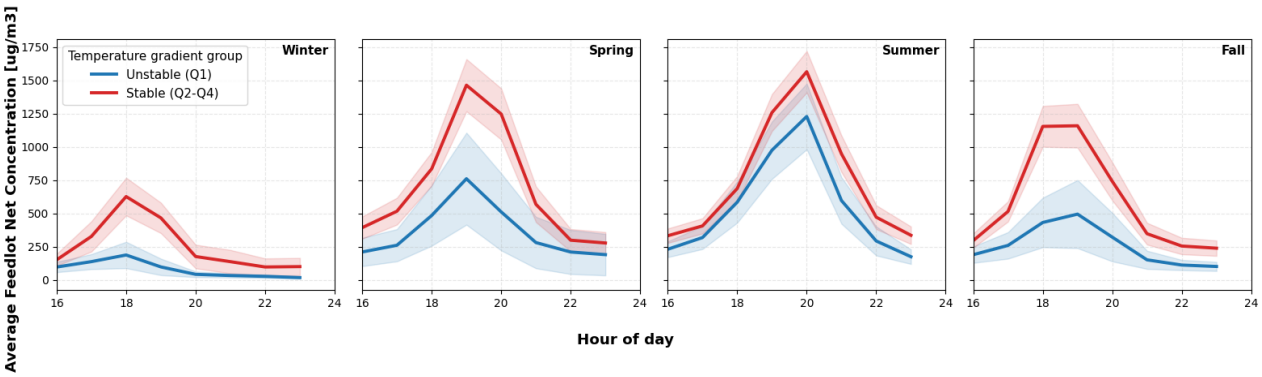

Figure 8. Effect of atmospheric stability on evening PM_{10} diurnal patterns by season showing threshold-based rather than linear response.

Table 1. Two-way ANOVA results testing the effects of atmospheric stability and modeled surface moisture on log-transformed evening PM_{10} concentrations.

Source of Variation	F-Value	p-value
Stability Group	111.75	< 0.001*
Modeled Surface Moisture	86.25	< 0.001*
Interaction	3.81	0.009

Table 2. Tukey's HSD post-hoc comparisons of surface moisture effects on log-transformed evening PM_{10} concentrations stratified by atmospheric stability regime.

Atmospheric Stability	Comparison (soil moisture grouping)	Mean Difference (Log)	p-value	Interpretation
Unstable	Q1 vs Q2	-0.66	0.158	No significant change
	Q1 vs Q3	-1.43	< 0.001*	Significant decrease
	Q1 vs Q4	**-2.53**	**< 0.001***	**Strongest decrease**
Stable	Q1 vs Q2	-0.15	0.968	No significant change
	Q1 vs Q3	-0.55	0.006*	Significant decrease
	Q1 vs Q4	**-1.69**	**< 0.001***	**Strong decrease**

4. Discussion

4.1 Long-Term EDP Trends: Validation and Methodological Considerations

The EDP magnitudes observed in this study are consistent with those reported in previous feedlot monitoring investigations (Bonifacio et al., 2012, 2011; Emert et al., 2024), with concentrations typically in the 1,000 μg/m³ range. It should be noted that the actual average values may be significantly higher than reported here, as concentrations were capped at 3,000 μg/m³ to prevent extreme outliers from distorting statistical analyses and visualizations. The seasonal concentration patterns observed in our dataset align with

findings reported in Guo et al. (2011b), in which dust concentrations were elevated during spring and summer months and lowest during winter (Habib et al., 2024; Purdy et al., 2007). Our 10-year continuous dataset advances the understanding established by Guo et al. (2011b) by demonstrating the remarkable consistency of elevated EDP contributions during summer months, where evening emissions accounted for 55–57% of the total daily 24-hour dust load across the entire study period (Figure 4). This sustained pattern across a decade of observations confirms that EDP is not merely an episodic phenomenon but rather a predictable and dominant feature of summer dust emission dynamics at feedlot operations.

However, several methodological considerations warrant discussion when interpreting these results. While winter data show low concentrations consistent with other studies, the unfavorable wind direction patterns during this season limit the number of valid measurement days available for analysis. The upwind-downwind TEOM array configuration requires southerly winds to capture net feedlot emissions, and as illustrated in Figure 2, up to 95% of potential measurement days during winter were unusable due to non-southerly wind conditions. This data limitation means that winter conclusions are necessarily drawn from a smaller and potentially non-representative sample of days, and caution should be exercised when generalizing winter EDP characteristics. This constraint highlights an inherent limitation of the upwind-downwind monitoring approach: while it provides accurate net emission measurements when wind conditions are favorable, it sacrifices temporal coverage in seasons or locations with variable wind patterns.

The consistent EDP trends documented in this study provide strong empirical support for the observation by Auvermann et al. (2010) that hourly PM_{10} concentrations can differ vastly from 24-hour average values. This finding carries important regulatory and public health implications. Feedlot operations that maintain compliance with the NAAQS 24-hour average limit of 150 $\mu g/m^3$ may nonetheless be generating PM_{10} concentrations during evening hours that exceed that level by factors of 10. Neighbors located immediately downwind of feedlot operations could therefore experience short-term exposure to PM_{10} levels well above regulatory limits during these intensive evening periods, even when daily average concentrations remain within acceptable bounds.

4.2 Effectiveness of the empirical moisture model and potential for future development

The integration of surface moisture modeling with HDW provides a practical framework for predicting feedlot dust emission potential that builds upon established understanding of dust generation mechanisms. As noted by de Oro (2021) and Emert et al. (2023), dust emissions in semi-arid climates are driven by dried feedlot surface material that becomes pulverized through cattle movement and is subsequently transported by wind, making HDW an effective proxy for capturing both the drying (VPD, wind speed) and transport (wind speed, turbulence) components of dust generation. The systematic reduction in correlation strength between daily cumulative HDW and EDP magnitude across surface moisture quartiles (Figure 6) validates the moisture suppression effect previously documented by Guo et al. (2011b) and Razote et al. (2006), demonstrating that surface wetness fundamentally moderates the relationship between atmospheric drying potential and dust emissions.

This study advances previous feedlot dust prediction approaches by demonstrating that the moisture monitoring concept can be operationalized at field scale using automated weather station systems, requiring significantly less labor than traditional ground-truth feedlot surface sampling methods employed in earlier studies. This approach leverages a key advantage of HDW: the required meteorological inputs (wind speed, temperature, relative humidity) can be measured easily with standard instrumentation, making the framework accessible (Srock et al., 2018). By coupling readily available meteorological observations with a simple recursive water balance model, this methodology provides continuous monitoring capability that was logistically infeasible in previous intensive sampling campaigns.

However, the varying predictive performance of HDW across moisture conditions reveals both challenges and opportunities for future model refinement. Under the driest surface conditions (Q1, Figure 6), HDW explained 43% of the variance in evening PM_{10} concentrations, demonstrating reasonable predictive capability when atmospheric drying demand is the primary driver of emission potential. Conversely, under the wettest conditions (Q4), HDW explained only 10% of the variance, indicating that when surface moisture effectively suppresses emissions, HDW become less determinative of dust concentrations. Notably, even under modeled wet surface conditions (Q4, Figure 6), observed evening PM_{10} concentrations occasionally reached 1,200 $\mu g/m^3$, suggesting that factors beyond surface moisture and atmospheric drying potential contribute substantially to emission variability. This finding underscores that while meteorological variables provide essential context for dust emission potential, comprehensive prediction models capable of informing operational decisions (such as timing of manure harvesting

or deployment of dust suppression measures) will require integration of additional information beyond weather data alone.

4.3 Effects of Atmospheric Stability on Evening Dust Concentrations

The relationship between temperature gradient and dust concentration observed in this study parallels findings from Muñoz and Corra (2017), who reported a positive correlation between temperature gradient and average PM_{10} concentration in urban pollution context. However, our analysis reveals a more nuanced relationship than simple linear correlation. In our study, the highest temperature gradient quartile (representing the strongest temperature inversions) does not correspond to the highest PM_{10} concentration group, indicating that inversion strength and dust concentration are not proportionally related. Instead, the data suggests that atmospheric stability operates more as a threshold phenomenon: the presence or absence of temperature inversion appears more critical than its magnitude. Specifically, conditions with weak or non-existent temperature inversions (particularly evident in winter and fall patterns shown in Figure 8) significantly reduce PM_{10} concentrations by promoting upward dispersion and vertical mixing of emitted dust particles, preventing their accumulation in the boundary layer near the surface.

The temporal relationship between EDP occurrence and maximum temperature inversion development provides additional insights into the relative importance of atmospheric stability versus emission source strength. If atmospheric trapping were the sole or dominant mechanism, concentration would be expected to remain elevated as long as stable conditions persisted, rather than declining while inversions are still present.

Additional evidence supporting animal activity as the principal emission driver comes from the consistent early-morning concentration minimum observed across seasons. During the period between 02:00 and 04:00, summer, fall, and winter all exhibit significant drops in PM_{10} concentrations (Figures 6) despite the continued presence of temperature inversions during these nocturnal hours, a trend similarly reported by Mitloehner et al. (2017). This pattern indicates that when cattle become inactive during their resting period, dust emissions decline to baseline levels regardless of atmospheric stability conditions that would otherwise trap any emitted particulates. Conversely, during morning hours when temperature inversions transition dramatically to unstable conditions at sunrise, PM_{10} concentrations do not decrease proportionally and typically remain relatively stable throughout this period of rapid atmospheric change. The data supports a conceptual model in which animal activity governs emission rates, while atmospheric stability modulates the degree to which those emissions accumulate at ground level instead of dispersing vertically.

5. Conclusion

This study makes contributions to understanding and predicting feedlot dust emissions, with implications for both scientific advancement and operational management. First, the comprehensive 10-year dataset confirms that 24-hour average PM_{10} concentrations inadequately represent feedlot dust dynamics for modeling and management purposes. EDP consistently contributes 40 to 50% of total daily dust loads across all seasons, with summer months showing even higher contributions exceeding 50%. This disproportionate emission contribution underscores the necessity of studying EDP

specific mechanisms and developing targeted mitigation strategies to reduce dust emissions during these critical periods.

Second, this research establishes a methodological foundation for using meteorological data to monitor feedlot surface moisture content and inform dust management decisions. By adapting the Hot Dry Windy Index originally developed for wildfire weather prediction to feedlot dust emission contexts, we demonstrated that readily available meteorological parameters (wind speed, temperature, and relative humidity) can be synthesized to characterize atmospheric drying potential and its interaction with surface moisture conditions. The primary strength of this approach lies in its operational feasibility: HDW can be calculated from standard weather station observations without requiring labor intensive field sampling campaigns. This study effectively bridges the gap between laboratory scale findings (demonstrating that surface moisture suppresses dust emissions) and field scale applications by providing a practical framework for translating basic meteorological observations into continuous estimates of feedlot dust emission potential. The empirical water balance model developed here represents a first step toward operational dust prediction tools that can support proactive management interventions.

Third, our analysis of atmospheric stability effects advances understanding of the physical mechanisms governing EDP occurrence and magnitude. The results demonstrate that atmospheric stability, characterized by vertical temperature gradients, cannot independently generate elevated evening dust concentrations. Rather, temperature inversions act as a modulating factor that traps emitted particulates near the surface once emissions have been generated by source activities. The temporal patterns observed

provide compelling evidence that animal activity represents the primary driver of dust emissions, while atmospheric stability determines the degree to which those emissions accumulate at ground level. This finding has important implications for future research directions: robust feedlot dust prediction algorithms capable of supporting operational management decisions will require integration of animal behavior data alongside meteorological information.

ORCID

Sirapoom Peanusaha https://orcid.org/0009-0002-4746-063X

Guillermo Marcillo https://orcid.org/0000-0002-5343-1088

Brent W. Auvermann https://orcid.org/0000-0001-6506-2921

Acknowledgement

This research is supported by Texas A&M AgriLife Research.

CRediT authorship contribution statement

Sirapoom Peanusaha: Conceptualization, Methodology, Software, Formal Analysis, Investigation, Writing – Original Draft, Writing – Review & Editing.

Guillermo Marcillo: Validation, Data Curation, Writing – Review & Editing, Supervision, Funding Acquisition.

Brent Auvermann: Conceptualization, Resources, Data Curation, Writing – Review & Editing, Supervision, Funding Acquisition.

Declaration of Generative AI and AI-assisted Technologies in the Writing Process

During the preparation of this work the authors used Google Scholar Labs, Claude, and ChatGPT in order to search literature, refining analytical scripts, edit, and grammar-check, the original manuscript provided. After using this tool/service, the author(s) reviewed and edited the content as needed and took full responsibility for the content of the publication.

Declaration of Competing Interest

The authors declare that they have no known competing financial interests or personal relationships that could have appeared to influence the work reported in this paper.

Reference

Arias-Pérez, R.D., Taborda, N.A., Gómez, D.M., Narvaez, J.F., Porras, J., Hernandez, J.C., 2020. Inflammatory effects of particulate matter air pollution. Environ Sci Pollut Res 27, 42390–42404. https://doi.org/10.1007/s11356-020-10574-w

Auvermann, B.W., Jack Bush, Gary Marek, Kevin Heflin, Brad Wilhite, Sharon L. P Sakirkin, 2010. Time-Varying PM10 Emissions from Open-Lot Dairies and Cattle Feedyards, in: International Symposium on Air Quality and Manure Management for Agriculture Conference Proceedings, 13-16 September 2010, Dallas, Texas. Presented at the International Symposium on Air Quality and Manure Management for Agriculture Conference Proceedings, 13-16 September 2010, Dallas, Texas, American Society of Agricultural and Biological Engineers. https://doi.org/10.13031/2013.32652

Bonifacio, H., Maghirang, R., Auvermann, B., Razote, E., Murphy, J., Harner, J., 2012. Particulate matter emission rates from beef cattle feedlots in Kansas-Reverse dispersion modeling. JOURNAL OF THE AIR & WASTE MANAGEMENT ASSOCIATION 62, 350–361. https://doi.org/10.1080/10473289.2011.651557

Bonifacio, H., Maghirang, R., Razote, E., Auvermann, B., Harner, J., Murphy, J., Guo, L., Sweeten, J., Hargrove, W., 2011. PARTICULATE CONTROL EFFICIENCY OF A WATER SPRINKLER SYSTEM AT A BEEF CATTLE FEEDLOT IN KANSAS. TRANSACTIONS OF THE ASABE 54, 295–304.

Bonifacio, H., Maghirang, R., Razote, E., Trabue, S., Prueger, J., 2013a. Comparison of AERMOD and WindTrax dispersion models in determining PM10 emission rates from a beef cattle feedlot. JOURNAL OF THE AIR & WASTE MANAGEMENT ASSOCIATION 63, 545–556. https://doi.org/10.1080/10962247.2013.768311

Bonifacio, H., Maghirang, R., Trabue, S., McConnell, L., Prueger, J., Razote, E., 2013b. Particulate Emissions from a Beef Cattle Feedlot Using the Flux-Gradient Technique. JOURNAL OF ENVIRONMENTAL QUALITY 42, 1341–1352. https://doi.org/10.2134/jeq2013.04.0129

Bush, K.J., Heflin, K., Marek, G., Bryant, T., Auvermann, B.W., 2014. Increasing Stocking Density Reduces Emissions of Fugitive Dust from Cattle Feedyards. Appl. Eng. Agric. 815–824. https://doi.org/10.13031/aea.30.10681

de Oro, L.A.A., Fernando; Panebianco, Juan Esteban; Buschiazzo, Daniel Eduardo, 2021. PM10 emission from feedlots in soils with different texture: Cattle trampling effect. Aeolian Research 53, 100742-NA. https://doi.org/10.1016/j.aeolia.2021.100742

Diller, L., Thompson, L., Blasi, D.A., Larson, H.E., 2026. Use of Unmanned Aerial Vehicle Technologies with Thermal Imaging to Assess Surface Moisture in Pens of Cattle Offered Energy-dense vs. Low-energy Feeding Programs.

Emert, A.D., Griffis-Kyle, K., Green, F.B., Smith, P.N., 2023. Atmospheric transport of particulate matter and particulate-bound agrochemicals from beef cattle feedlots: Human health implications for downwind agricultural communities. Science of The Total Environment 894, 164678. https://doi.org/10.1016/j.scitotenv.2023.164678

Emert, A.D., Griffis-Kyle, K., Portillo-Quintero, C., Smith, P.N., 2024. USEPA CALPUFF validation and dispersion modeling of beef cattle feedlot PM10 and PM2.5

emissions factors. Atmospheric Environment 316, 120189. https://doi.org/10.1016/j.atmosenv.2023.120189
Feng, Y., Sun, F.-B., Wang, H., Liu, F., 2026. Increasing coupling of hot–dry winds and drought across China: Observational evidence and future projection. Advances in Climate Change Research 17, 91–104. https://doi.org/10.1016/j.accre.2025.10.011
Guo, L., Maghirang, R., Razote, E., Auvermann, B., 2011a. Laboratory Evaluation of Dust-Control Effectiveness of Pen Surface Treatments for Cattle Feedlots. JOURNAL OF ENVIRONMENTAL QUALITY 40, 1503–1509. https://doi.org/10.2134/jeq2010.0520
Guo, L., Maghirang, R., Razote, E., Trabue, S., McConnell, L., 2011b. Concentrations of Particulate Matter Emitted from Large Cattle Feedlots in Kansas. JOURNAL OF THE AIR & WASTE MANAGEMENT ASSOCIATION 61, 1026–1035. https://doi.org/10.1080/10473289.2011.599282
Habib, M.R., Arzadon, E., Capareda, S., 2024. Particulate matter annual emission factors for dairy facilities and cattle feedlots of Texas, USA. Atmospheric Environment 328, 120519. https://doi.org/10.1016/j.atmosenv.2024.120519
Hiranuma, N., Brooks, S.D., Gramann, J., Auvermann, B.W., 2011. High concentrations of coarse particles emitted from a cattle feeding operation. Atmos. Chem. Phys. 11, 8809–8823. https://doi.org/10.5194/acp-11-8809-2011
Jones, D., Guerrero, B., Pinero, J., 2024. The Impact of Agribusiness in the High Plains Trade Area. Amarillo Chamber of Commerce, Amarillo, TX.
Lepot, M., Aubin, J.-B., Clemens, F., 2017. Interpolation in Time Series: An Introductive Overview of Existing Methods, Their Performance Criteria and Uncertainty Assessment. Water 9, 796. https://doi.org/10.3390/w9100796
Loneragan, G.H., Dargatz, D.A., Morley, P.S., Smith, M.A., 2001. Trends in mortality ratios among cattle in US feedlots. javma 219, 1122–1127. https://doi.org/10.2460/javma.2001.219.1122
MacVean, D.W., Franzen, D.K., Keefe, T.J., Bennett, B.W., 1986. Airborne particle concentration and meteorologic conditions associated with pneumonia incidence in feedlot cattle. ajvr 47, 2676–2683. https://doi.org/10.2460/ajvr.1986.47.12.2676
Marcillo, G.S., Auvermann, B., 2025. A data repository of feedyard particulate matter emissions (PM10) in West Texas, US. Data in Brief 63, 112168. https://doi.org/10.1016/j.dib.2025.112168
Marek, G., 2006. Determination of Feedyard Evaporation Using Weighing Lysimeters. West Texas A&M University.
McDonald, J.M., Srock, A.F., Charney, J.J., 2018. Development and Application of a Hot-Dry-Windy Index (HDW) Climatology. Atmosphere 9, 285. https://doi.org/10.3390/atmos9070285
McGinn, S.M., Flesch, T.K., Chen, D., Crenna, B., Denmead, O.T., Naylor, T., Rowell, D., 2010. Coarse Particulate Matter Emissions from Cattle Feedlots in Australia. J of Env Quality 39, 791–798. https://doi.org/10.2134/jeq2009.0240
Mitloehner, F., Dailey, J., Morrow, J., McGlone, J., 2017. Impact of Feed Delivery Pattern on Aerial Particulate Matter and Behavior of Feedlot Cattle †. Animals 7, 14. https://doi.org/10.3390/ani7030014

Monteith, J.L., Unsworth, M.H., 2013. Principles of environmental physics: plants, animals, and the atmosphere, 4th edition. ed. Elsevier/Academic Press, Amsterdam Boston.
Mukherjee, A., Agrawal, M., 2017. World air particulate matter: sources, distribution and health effects. Environ Chem Lett 15, 283–309. https://doi.org/10.1007/s10311-017-0611-9
Muñoz, R.C., Corral, M.J., 2017. Surface Indices of Wind, Stability, and Turbulence at a Highly Polluted Urban Site in Santiago, Chile, and their Relationship with Nocturnal Particulate Matter Concentrations. Aerosol Air Qual. Res. 17, 2780–2790. https://doi.org/10.4209/aaqr.2017.05.0190
Olofson, K.F.G., Andersson, P.U., Hallquist, M., Ljungström, E., Tang, L., Chen, D., Pettersson, J.B.C., 2009. Urban aerosol evolution and particle formation during wintertime temperature inversions. Atmospheric Environment 43, 340–346. https://doi.org/10.1016/j.atmosenv.2008.09.080
Purdy, C.W., Clark, R.N., Straus, D.C., 2007. Analysis of Aerosolized Particulates of Feedyards Located in the Southern High Plains of Texas. Aerosol Science and Technology 41, 497–509. https://doi.org/10.1080/02786820701225838
Razote, E., Maghirang, R., Predicala, B., Murphy, J., Auvermann, B., Harner, J., Hargrove, W., 2006. Laboratory evaluation of the dust-emission potential of cattle feedlot surfaces. TRANSACTIONS OF THE ASABE 49, 1117–1124.
Razote, E.B., Maghirang, R.G., Guo, L., Tallada, J.G., Auvermann, B.W., Iii, J.P.H., Hargrove, W.L., 2008. TEOM Measurements of PM10 and PM2.5 Concentrations at Cattle Feedlots in Kansas, in: Mid-Central Conference. Presented at the Mid-Central Conference, American Society of Agricultural and Biological Engineers. https://doi.org/10.13031/2013.25206
Srock, A.F., Charney, J.J., Potter, B.E., Goodrick, S.L., 2018. The Hot-Dry-Windy Index: A New Fire Weather Index. Atmosphere 9, 279. https://doi.org/10.3390/atmos9070279
Sweeten, J., Parnell, C., Shaw, B., Auvermann, B., 1998. Particle size distribution of cattle feedlot dust emission. TRANSACTIONS OF THE ASAE 41, 1477–1481.
Urso, P.M., Turgeon, A., Ribeiro, F.R.B., Smith, Z.K., Johnson, B.J., 2021. Review: the effects of dust on feedlot health and production of beef cattle. Journal of Applied Animal Research 49, 133–138. https://doi.org/10.1080/09712119.2021.1903476
USEPA, 2024. Final Rule to Strengthen the National Air Quality Health Standard for Particulate Matter Fact Sheet.
WMO Guidelines on the Calculation of Climate Normals_en, 2017.
Zhang, Y., Li, X., Wei, W., Chen, C., 2025. Characteristics of consecutive hot-dry-windy events with different severities in China. Journal of Hydrology 662, 133982. https://doi.org/10.1016/j.jhydrol.2025.133982